

The galaxy luminosity function in clusters and the field

Neil Trentham

Institute for Astronomy, University of Hawaii
2680 Woodlawn Drive, Honolulu HI 96822, U. S. A.
email : nat@newton.ifa.hawaii.edu

Submitted to *MNRAS*

ABSTRACT

We present the results from a CCD survey of the B -band luminosity functions of nine clusters of galaxies, and compare them to published photographic luminosity functions of nearby poor clusters like Virgo and Fornax and also to the field luminosity function. We derive a composite luminosity function by taking the weighted mean of all the individual cluster luminosity functions; this composite luminosity function is steep at bright and faint magnitudes and is shallow in-between.

All clusters have luminosity functions consistent with this single composite function. This is true both for rich clusters like Coma and for poor clusters like Virgo.

This same composite function is also individually consistent with the deep field luminosity functions of Cowie et al. (1996) and Ellis et al. (1996), and also with the faint-end of the Las Campanas Redshift Survey R -band luminosity function, shifted by 1.5 magnitudes. A comparison with the Loveday et al. (1992) field luminosity function which is well-determined at the bright-end, shows that the composite function that fits the field data well fainter than $M_B = -19$ drops too steeply between $M_B = -19$ and $M_B = -22$ to fit the field data there well.

Key words: galaxies: luminosity function – galaxies: clusters: luminosity function

1 INTRODUCTION

The galaxy luminosity function $\phi(L)$, defined as the number density of galaxies per unit luminosity, is one of the most direct observational probes of galaxy formation theories.

Most evidence (see references below) suggests that $\phi(L)$ drops steeply brighter than about $M_B = -21$ (i.e., extremely luminous galaxies are very rare), and rises more gradually fainter than this. This form is expressed well by the Schechter (1976) function. At very faint magnitudes $M_B > -10$, we expect on theoretical grounds that $\phi(L)$ turns over again, as we expect star formation in very low mass systems to be suppressed by photoionization of the intergalactic medium from the ultraviolet background (Efstathiou 1992, Chiba & Nath 1994, Thoul & Weinberg 1995), but this turnover has not yet been observed.

It is also well established that different types of galaxies contribute proportionately different amounts to $\phi(L)$ at different magnitudes. At bright magnitudes $M_B > -16$, most galaxies in clusters are giant ellipticals and in the field they are giant late-type galaxies. At fainter magnitudes $M_B < -16$, most galaxies in clusters are dwarf spheroidal galaxies (see Binggeli 1987 – note that he calls them dwarf ellipticals), and in the field, they are either dwarf spheroidal or dwarf spiral and irregular galaxies. The different types of galaxies have different scaling laws and they lie in different parts of the fundamental plane parameter correlation diagrams (Kormendy 1985, 1987, Binggeli 1994), suggesting that different physical processes are at work at producing their luminosities. There is however some overlap between the different types, particularly between dwarf irregular and dwarf spheroidal galaxies. That clusters and the field behave differently is thought to be due to the fact that in clusters, the crossing time is less than the Hubble time so that galaxies there will be influenced by cluster-related processes.

What all this suggests is that the physics controlling the total galaxy luminosity function is very complicated. Nevertheless $\phi(L)$ is a directly observable quantity, so it provides a popular and direct way to compare theory with observation.

Early attempts (e.g., White & Rees 1978) were successful at producing the general shape of $\phi(L)$. Recent theoretical advances (e.g. White & Kauffmann 1994, van Kampen 1995, Babul & Ferguson 1996) now allow us to calculate $\phi(L)$ in detail from first principles albeit with many assumptions and approximations and thereby constrain combinations of fundamental cosmological quantities. Much observational work in this subject has been done in both the field (e.g., Kirshner et al. 1983, Loveday et al. 1992, Marzke et al. 1994, Ellis et al. 1996, Cowie et al. 1996) and in clusters (e.g., Oemler 1974, Sandage et al. 1985, Lugger 1986, Oegerle & Hoessel 1989, Ferguson & Sandage 1991, plus several recent papers – see Section 2). This work provides a sound basis for comparison with theory.

Recent advances like the development of large-format CCDs, fibre-optic spectrographs, and the construction of the 10 m Keck telescopes, have allowed measurement of the galaxy luminosity down to very faint magnitudes with unprecedented accuracy in both galaxy clusters and in the field. In particular, measurements now go deep enough that we can begin to probe the part of $\phi(L)$ where the dwarf galaxies contribute significantly. Here we present a compilation of recent work at these faint limits and assess the case for a universal galaxy luminosity function.

Throughout this paper we assume that $H_0 = 75 \text{ km s}^{-1} \text{ Mpc}^{-1}$ and that $\Omega_0 = 1$.

2 OBSERVATIONS AND RESULTS

2.1 Clusters

Here we present the results of a study of the (Johnson) B -band luminosity functions of nine clusters with $0 < z < 0.2$, down to $M_B = -10$. This work uses various CCD cameras on the University of Hawaii 2.2 m Telescope and the Canada-France-Hawaii Telescope; the data and the details of its reduction and analysis are described elsewhere (Trentham 1997). Various specialized techniques have been used; these include a detailed characterization of the background number counts for $B < 26$ (see also Driver et al. 1994a, 1994b, Bernstein et al. 1995), and also techniques for measuring total magnitudes of galaxies that take into account their detailed seeing-convolved light distributions (Trentham 1996).

The clusters observed by us are: Abell 665 ($z = 0.18$), Abell 963 ($z = 0.21$), Abell 1146 ($z = 0.14$), Abell 1795 ($z = 0.06$), Abell 2199 ($z = 0.03$), Coma, Abell 1367, Abell 262, and the NGC 507 Group (all $z = 0.02$). For these clusters, and also for Virgo (Sandage et al. 1985), Fornax (Ferguson 1989), the Local Group (van den Bergh 1992), and a number of other nearby groups (Ferguson & Sandage 1991, Tully 1988), we computed a composite luminosity function. In this calculation, we adopt the error estimates given in the original sources, we normalize so that the total number of galaxies brighter than $M_B = -16$ in each cluster is the same, and we sum the luminosity functions. In effect, this is a weighted average of all the individual luminosity functions. We chose $M_B = -16$ as the normalization threshold because this is approximately where the dwarf-giant transition occurs in the fundamental plane (Kormendy 1987, Binggeli 1994). This calculation is therefore not sensitive to the dwarf-to-giant ratio or to the properties of the dwarf population.

The resulting composite luminosity function is presented in Table 1 and in Figure 1. The figure shows that $\phi(L)$ is steep at very bright magnitudes, $M_B < -20$ and also at faint magnitudes, $-14 < M_B < -11$. It is somewhat more shallow in between but it is still significantly steeper than $\alpha = -1$. The error bars are small enough that the curvature in this luminosity function is highly significant, and a power-law does not provide a good fit to the data over any significant magnitude range. Table 1 also lists the local slope (α , where $\phi(L) \propto L^\alpha$ and $N(M) = -\phi(L) \frac{dL}{dM} \propto 10^{-0.4(\alpha+1)M}$) of the luminosity function described by Figure 1. Here $-0.4(\alpha(M) + 1)$ is the best-fitting linear slope at M of the three points at $M - 1$, M , and $M + 1$. It is apparent from the numbers listed in Table 1 that $\alpha < -1$ everywhere; a flat composite luminosity function ($\alpha = -1$) is ruled out at any magnitude. We do not present a luminosity function fainter than $M_B = -11$, as we have measurements this faint only in Abell 1367 and Abell 262.

It is interesting that the luminosity function is continuous over the magnitude range where there is a break between giants and dwarfs in the fundamental plane ($M_B \sim -16$). Indeed, it is flatter in this transition region than anywhere else. This is suggestive of a conspiracy in which the giant galaxy luminosity function is falling as luminosity decreases by an amount almost exactly compensated for by the rise in the dwarf luminosity function.

Figure 2 shows how the average function presented in Figure 1 compares with the individual luminosity functions of each cluster. That the composite function fits all of the individual data sets so well is remarkable and provides a strong case for a universal luminosity function in clusters. Table 2 provides for each case the number of degrees of freedom ν and the reduced χ^2 of the composite luminosity function that is normalized to provide the best fit to the data, as well as the probability P of obtaining this value of χ^2 or lower if this luminosity function is the correct representation. Little significance should be attached to low numbers in the final column because the true errors are probably more

systematic than random. For example, the Tully and Ferguson-Sandage groups are biased towards points near $M_B = -20.5$, as these groups were identified by searching around such galaxies. Ignoring the $M_B = -20.5$ point improves the quality of the fit substantially. The fit in the Local Group is not good either, but given the combination of selection effects (the Sagittarius dwarf with $M_B \sim -13$ was discovered only two years ago; Ibata et al. 1994) and poor counting statistics, the quality of the fit does not have much significance.

Also apparent in comparing Figures 1 and 2 is that, at least for the more distant clusters ($z > 0.01$), the luminosity function is poorly constrained in each cluster (this is in part why the χ^2 values in Table 2.2 for these clusters are so low), but in combination the clusters constrain the composite function very tightly. This is because for each cluster, the uncertainties brought about by field-to-field variance in the subtracted background are high – it is only when we look at a large sample of these clusters in combination that the pattern shown in Figure 1 becomes clearly visible. Note also that the uncertainty $\Delta\alpha$ in deriving α for each cluster increases rapidly as α increases. Therefore, measuring α at the faint end based on the datasets we present for clusters like A665 and A963 is extremely difficult: we cannot even distinguish between $\alpha = -1.6$ and $\alpha = -1$ at the faint end (the value of the composite function here is $\alpha = -1.4$ at the faintest points). Only if $\alpha < -2$ in an individual cluster could we measure it so better than 0.1.

It is particularly intriguing that the luminosity functions of Virgo and Fornax are so well fit by the composite function at the faint end. The measurements of $\phi(L)$ in these nearby clusters come from photographic wide-field surveys (see Table 1 for references). The errors here come from counting statistics, not from a background subtraction, so they are much smaller than those for the more distant clusters. In Virgo, the faintest four points, which use the Impey et al. (1988) completeness corrections, are not used in deriving the composite function. The agreement between these points and the composite line is perhaps suggestive that the corrections are accurate. The case of Fornax is even more remarkable. The faintest three points were not used in computing the composite function, because we worried about surface-brightness selection effects like those described by Impey et al. (1988) in Virgo. Yet they agree very well with the composite function. Given the very small errors in the Fornax dataset (Ferguson 1989), we had no reason to expect χ^2 to be so low; we therefore suggest that the surface-brightness selection effects in the Fornax sample are small at the faint end, and, more importantly, that the composite function is in fact valid over a wide range of richness at faint magnitudes.

Although this paper only presents CCD observations of rich clusters from our own B -band survey (to ensure consistency in the photometry as well as to ensure consistency with the photographic and field data magnitude systems), a number of other papers have recently appeared on this subject to which the reader is referred (Thompson & Gregory 1993, Driver et al. 1994b, Biviano et al. 1995, De Propris et al. 1995, Bernstein et al. 1995, Secker & Harris 1996, Wilson et al. 1997). Many other authors find results similar to ours. The biggest differences are seen in A2199 (where we find a far shallower luminosity function than that seen by De Propris et al. 1995; this is because our field-to-field variance in the background more than an order of magnitude larger than theirs, so that our uncertainty in the faintest points, which define their slope, is much larger) and A665 (where the large number of faint galaxies predicted by the completeness model of Wilson et al. 1997 are not seen in our deeper data). Smaller discrepancies are seen in A963 (where we use a more generalized method of making isophotal corrections than Driver et al. 1994 which leads us to measure larger total magnitudes for the faintest galaxies and so derive a shallower slope)

and Coma (where we find more galaxies in our data at the faint end than predicted by the completeness model of Secker & Harris 1996). It is encouraging, however, that the database of cluster luminosity functions is growing, particularly at high redshift, where the galaxy population in clusters (Butcher & Oemler 1978, 1984; Dressler et al. 1994) is quite different to that at $z = 0$.

2.2 Field

We therefore have a composite luminosity function which seems to provide very good fits to the data in both rich clusters like Coma and poor clusters like Virgo and Fornax. Next we investigate how well it fits the field data, and compare it to the two deepest datasets (the Autofib dataset of Ellis et al. 1996, and the Keck dataset of Cowie et al. 1996). We also compare it to the Loveday et al. (1992) sample, which covers much more area than the deep samples, but does not sample such faint absolute magnitudes.

Figure 3 shows how our composite cluster function compares to the field data. We find that our function is consistent with either the Cowie et al. data or the Autofib data, but with different normalizations that are inconsistent with each other at the 3σ confidence level. The issue of the normalization of the field luminosity function is complicated (see e.g. Colless 1995 and references therein, Heyl et al. 1996, Lin et al. 1996) and there may be many explanations for what is seen here, for example clustering and large-scale structure along the line of sight. One of the classical problems (Colless 1995) of the field surveys was their bias towards high surface-brightness galaxies; this is unlikely to be a problem for the deep field surveys here as they detect galaxies with lower surface-brightnesses than the faintest galaxies in the cluster sample.

We also compare our luminosity function with the Las Campanas Redshift Survey luminosity function of Lin et al. (1996). This is the largest field-survey to date, comprising 18678 galaxies, reaching $M_R = -16$. We do not present in Figure 3 because of the different filter systems (it is in the R -band, whereas our data and the other surveys are in the B -band). For the Lin et al. sample, in the range $-18 < M_R < -16$ (approximately $-16.5 < M_B < -14.5$), a power-law fit to their luminosity function gives $\alpha = -1.39 \pm 0.11$, which is consistent with the value $\alpha = -1.43$ in this magnitude range for the cluster composite function (see Table 1). However, there is some evidence the Lin et al. luminosity function flattens at their very faint-end: for $-17.5 < M_R < -16$, a power-law fit gives $\alpha = -1.19 \pm 0.19$. If this trend continues to fainter magnitudes $-16 > M_R > -12$, the field and cluster luminosity functions would then be incompatible. There is weak evidence for this from the Local Group luminosity function, but this might simply be due to completeness effects.

In summary, at the faint-end, the composite cluster luminosity function has a shape consistent with those of the Cowie et al., Ellis et al., and Lin et al. field luminosity functions. However, the statistics in the field samples are at present poor, so that the case for a universal luminosity function at faint magnitudes cannot be addressed rigorously at present.

In comparison with the Loveday et al. (1992) field luminosity function which has excellent statistics at the bright-end, the composite function that fits the data well fainter than $M_B = -19$ drops too steeply between $M_B = -19$ and $M_B = -22$ to fit the field data there well. This could be because massive late-type galaxies whose dominated by young stellar populations, exist in the field but not in clusters because cluster-related process like gas stripping have turned off star formation there. We see this effect in the B -band because the B -band light of a galaxy primarily comes from the young stars. There may also be

a deficiency of star-forming galaxies in clusters at fainter magnitudes, but this does not cause a noticeable difference in the luminosity function, because it is much flatter there, and because the field statistics are worse. We also note that the bright-end slope of the rich-cluster luminosity function is slightly steeper than that of the poor-cluster luminosity function (Figure 4), which could also be due to the same effect.

ACKNOWLEDGMENTS

Helpful discussions with Len Cowie and John Kormendy are gratefully acknowledged.

I also thank Richard Ellis and the staff of the Institute of Astronomy in Cambridge for their hospitality during 1996, when most of this work was carried out.

This research has made use of the NASA/IPAC extragalactic database (NED) which is operated by the Jet Propulsion Laboratory, Caltech, under agreement with the National Aeronautics and Space Administration.

REFERENCES

- Abell G. O., 1958, *ApJS*, 3, 211
Babul A., Ferguson H. C., 1996, *ApJ*, 458, 100
Bernstein G. M., Nichol R. C., Tyson J. A., Ulmer M. P., Wittman D., 1995, *AJ*, 110, 1507
Binggeli B., 1987, in Faber S. M., ed., *Nearly Normal Galaxies*. Springer-Verlag, New York, p. 195
Binggeli B., 1994, in Meylan G., Prugneil P., ed., *ESO Conference and Workshop Proceedings No. 49: Dwarf Galaxies*. European Space Observatory, Munich, p. 13
Binggeli B., Sandage A., Tamman G. A., 1988, *ARAA*, 26, 509
Biviano A., Durret F., Gerbal D., Le Fevre O., Lobo C., Mazure A., Slezak E., 1995, *A&A*, 297, 610
Butcher H. R., Oemler, A., 1978, *ApJ*, 219, 18
Butcher H., Oemler A., 1984, *ApJ*, 285, 426
Chiba M., Nath B. B., 1994, *ApJ*, 436, 618
Coleman G. D., Wu C-C., Weedman D. W., 1980, *ApJS*, 43, 393
Colless M., 1995 in Maddox S. J., Aragón-Salamanca., ed., *Wide-Field Spectroscopy and the Distant Universe*, proceedings of the 35th Herstmonceux Conference, World Scientific, Singapore, p. 263
Cowie L. L., Songaila A., Hu E. M., Cohen J. G., 1996, *AJ*, 112, 839
De Propris R., Pritchet C. J., Harris W. E., McClure R. D., 1995, *ApJ*, 450, 534
Dressler, A., Oemler A., Sparks W. B., Lucas R. A., 1994, *ApJ*, 435, L23
Driver S. P., Phillipps S., Davies J. I., Morgan I., Disney M. J., 1994a, *MNRAS*, 266, 155
Driver S. P., Phillipps S., Davies J. I., Morgan I., Disney M. J., 1994b, *MNRAS*, 268, 393
Efstathiou G., 1992, *MNRAS*, 256, 43p
Ellis R. S., Colless M., Broadhurst T., Heyl J., Glazebrook K., 1996, *MNRAS*, 280, 235
Ferguson H. C., 1989, *AJ*, 98, 367
Ferguson H. C., Sandage A., 1991, *AJ*, 101, 765
Heyl J., Colless M., Ellis R. S., Broadhurst T., 1996, *MNRAS*, in press
Hodge P. W., 1989, *ARAA*, 27, 139
Ibata R. A., Gilmore G., Irwin M. J., 1994, *Nat*, 370, 194
Impey C., Bothun G., Malin D., 1988, *ApJ*, 330, 634

Kirshner R. P., Oemler A., Schechter P. L., Shectman S. A., 1983, AJ, 88, 1285
 Kormendy J., 1985, ApJ, 295, 73
 Kormendy J., 1987, in Faber S. M. ed., *Nearly Normal Galaxies*. Springer-Verlag, New York, p. 163
 Lin H., Kirshner R. P., Shectman S. A., Landy S. D., Oemler A., Tucker D. L., Schechter P. L., 1996, ApJ, 464, 60
 Loveday J., Peterson B. A., Efstathiou G., Maddox S., 1992, ApJ, 390, 338
 Lugger P., 1986, ApJ, 303, 535
 Maddox S. J., Efstathiou G., Sutherland W. J., 1990, MNRAS, 246, 433
 Marzke R. O., Geller M. J., Huchra J. P., Corwin H. G., 1994, AJ, 108, 437
 Metcalfe N., Fong R., Shanks T., 1995, MNRAS, 274, 769
 Oegerle W. R., Hoessel J. G., 1989, AJ, 98, 1523
 Oemler A., 1974, ApJ, 194, 1
 Sandage A., Binggeli B., Tammann G. A., 1985, AJ, 90, 1759
 Schechter P., 1976, ApJ, 203, 297
 Secker J., Harris W. E., 1996, ApJ, 469, 623
 Thompson L. A., & Gregory S. A., 1993, AJ, 106, 2197
 Thoul A. A., Weinberg D. H., 1995, ApJ, 442, 480
 Trentham N., 1996, MNRAS, in press
 Trentham N., 1997, PhD Thesis, University of Hawaii
 Tully R. B., 1988, AJ, 96, 73
 van den Bergh S., 1992, A&A, 264, 75
 van Kampen E., 1995, MNRAS, 273, 295
 White S. D. M., Kauffmann G., in Munoz-Tunon C., Sanchez F., eds., *The Formation and Evolution of Galaxies*. Cambridge University Press, Cambridge, p. 455
 White S. D. M., Rees M. J., 1978, MNRAS, 183, 321
 Wilson G., Smail I., Ellis R. S., Couch W. J., 1997, MNRAS, in press

FIGURE CAPTIONS

Figure 1. The composite cluster luminosity function computed as described in the text and in Table 1. Here $N_{\text{gal}} \propto \phi(M) = \phi(L) \frac{dL}{dM}$ is the number of galaxies per unit area per unit magnitude; it is arbitrarily normalized to represent the number of galaxies in a typical Abell (1958) richness 2 cluster.

Figure 2. Comparison between each cluster luminosity function and the composite function. The lines are the function in Table 1 and Figure 1, normalized for each cluster to minimize the scatter with the data for $M_B > -22$. In each diagram the data comes from the source listed in Table 1. In each case the errors bars are a combination of the uncertainties from counting statistics, field-to-field variance in the background (if a background subtraction is made), and uncertainties in the galaxy magnitudes; the reader is referred to the original sources for details. The two lines near the top center in each figure represent the slopes $\alpha = -1$ (solid line) and $\alpha = -2$ (dotted line). In the Virgo plot, the open circles represent data faintward of the completeness limit of Sandage et al. (1985). These are data points computed by Impey et al. (1988) using the Sandage data set with completeness corrections appropriate to their $\mu_{\text{lim}} = 25.8$ model. For the Ferguson-Sandage groups and the Tully

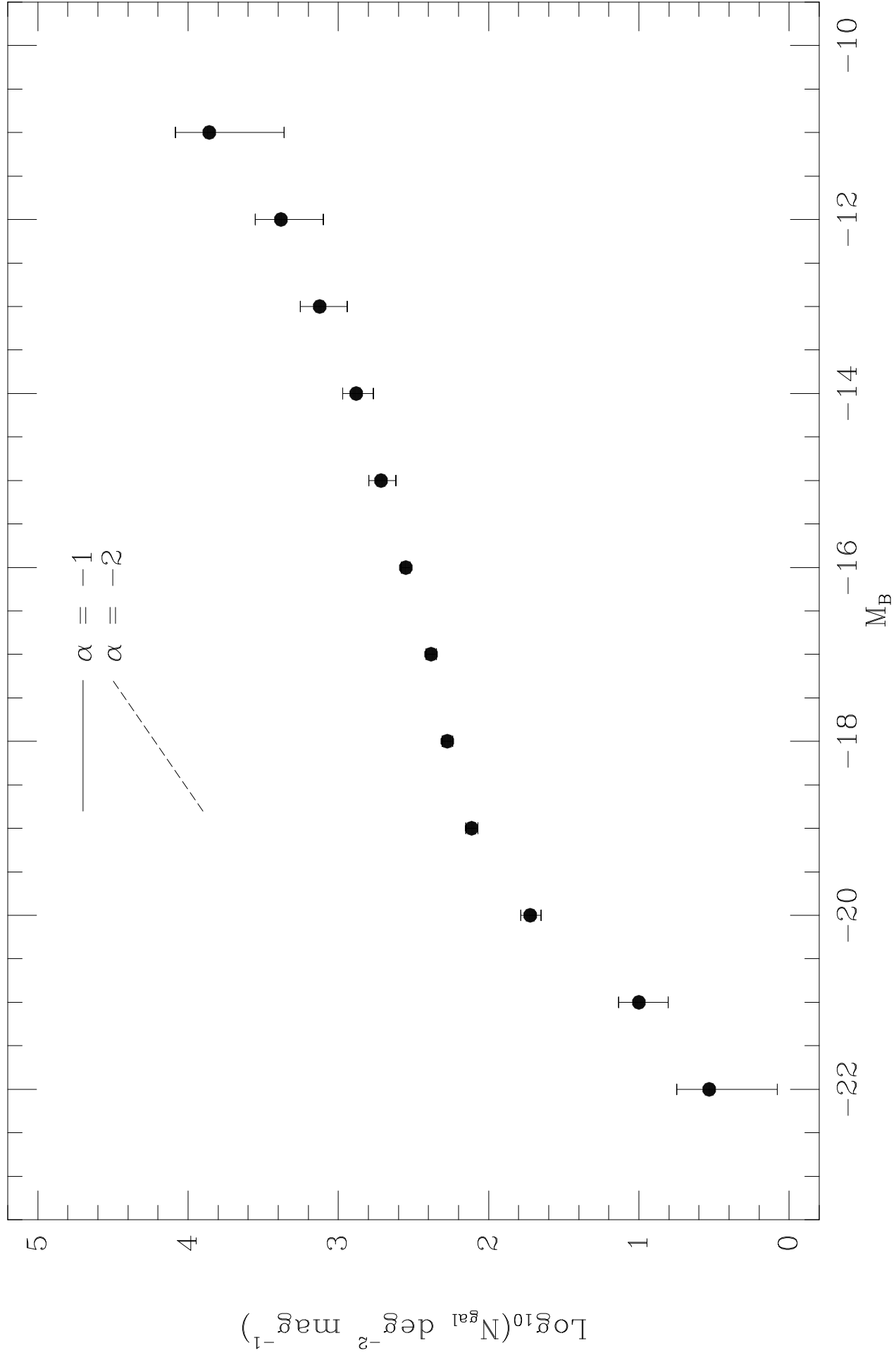
groups, the solid lines represent the composite function normalized to all the data, and the dashed lines represent the function normalized to the data minus to $M_B = -20.4$ (Ferguson-Sandage) or $M_B = -20.5$ (Tully) points. In the Local Group, only data brightward of the Sagittarius dwarf completeness limit (marked S in the diagram) are included in computing the normalization.

Figure 3. The field luminosity functions of Cowie et al. (1996), Ellis et al. (1996 – the Autofib survey), and Loveday et al. (1992). The composite luminosity functions normalized to minimize the scatter with the Cowie, Autofib, and Loveday (for $M_B > -21$ only) data are also presented. Symbols and line styles are as given in the figure legend.

The b_J data of Ellis et al. and Loveday et al. have been converted to the B band using the equation $b_J = B - 0.28(B - V)$ (Maddox et al. 1990, see also Metcalfe et al. 1995), the local galaxy type distribution as a function of absolute magnitude in the field of Binggeli et al. (1988), and the zero redshift colours of different galaxy types of Coleman et al. (1980). These corrections are typically 0.1 – 0.3 magnitudes.

Figure 4. The slope of the luminosity function at $M_B = -20$, computed as described in the text, as a function of the local galaxy density. The absolute values of the density are somewhat arbitrary as different angular regions of different clusters are surveyed. Nevertheless we do see a positive correlation at a weak level as described in the text.

For the rich clusters, a weighted average of the slopes and densities for Coma, Abell 1146, Abell 963, and Abell 665 is used. For the poor clusters, a weighted average of the slopes and densities for Virgo and Fornax is used. The solid line represents the slope of the Loveday et al. field luminosity function, computed the same way, and the dotted lines its 1σ uncertainty.



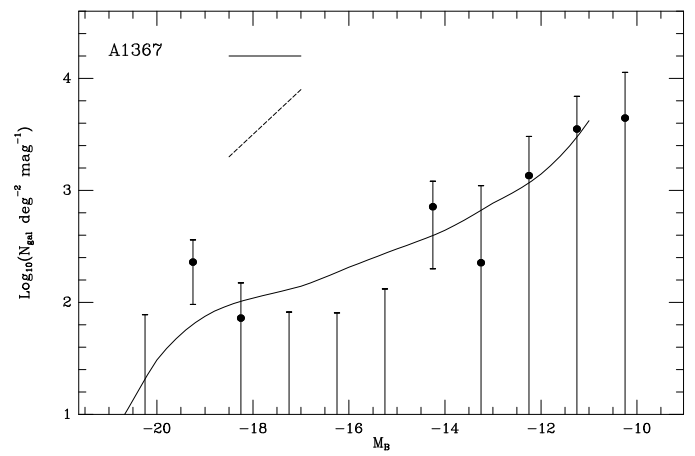
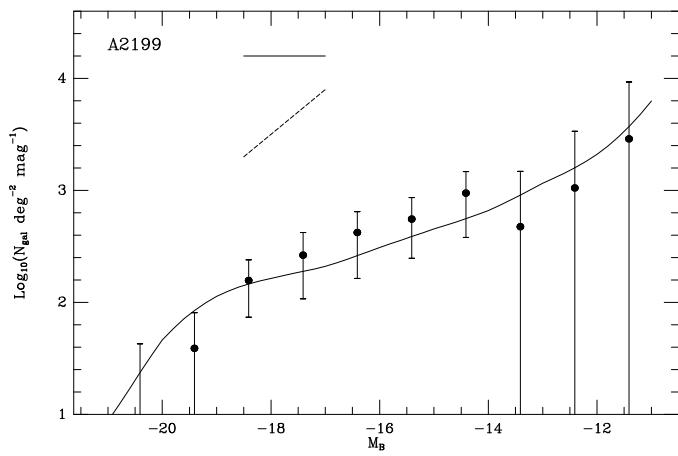
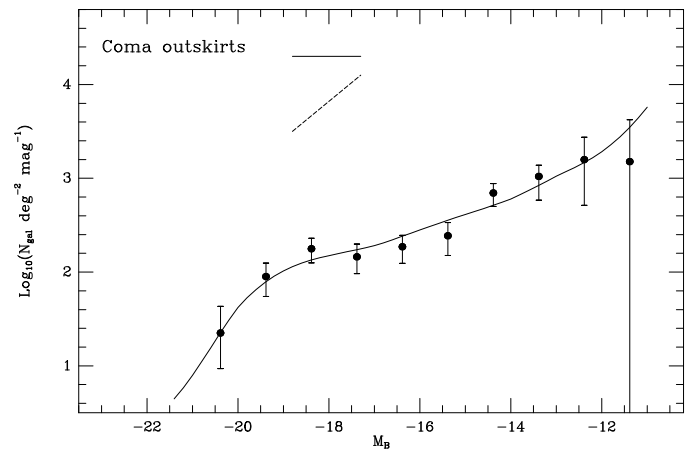
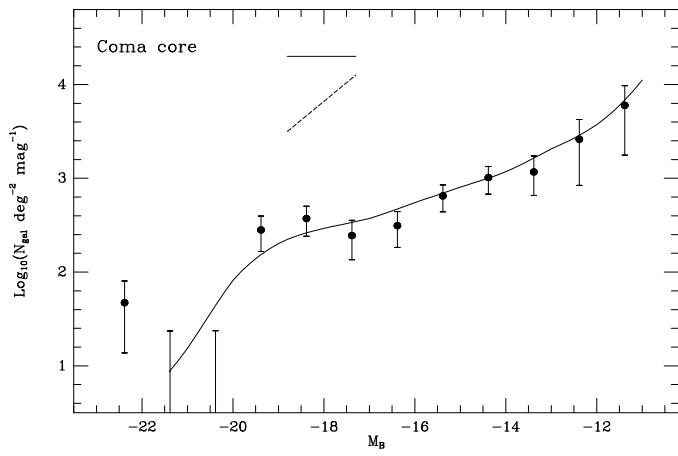
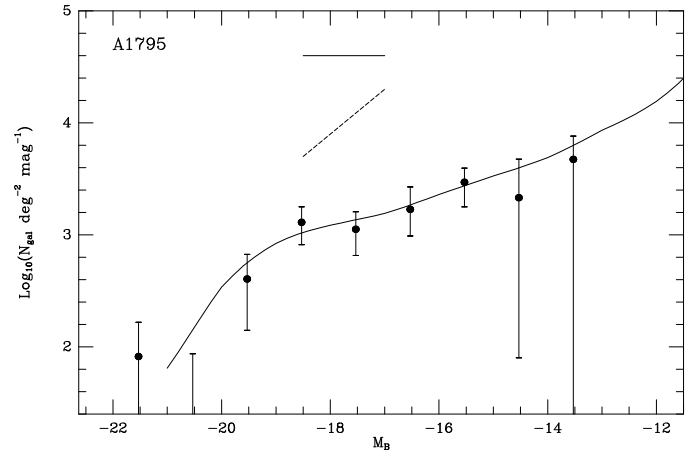
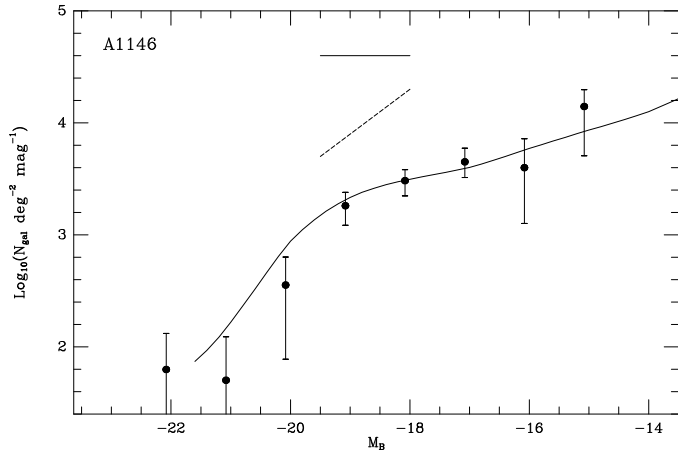
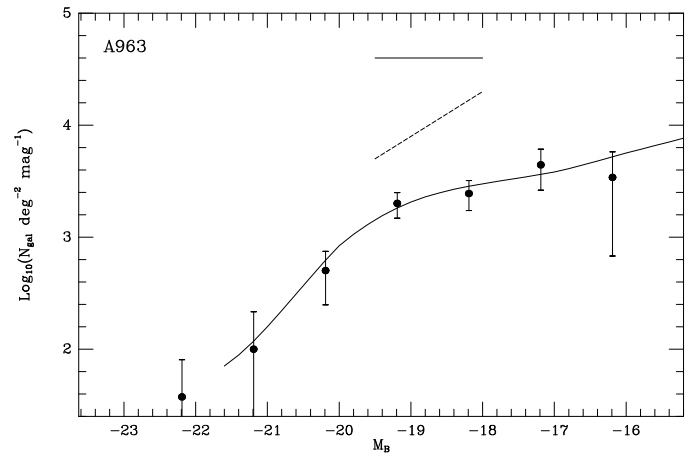
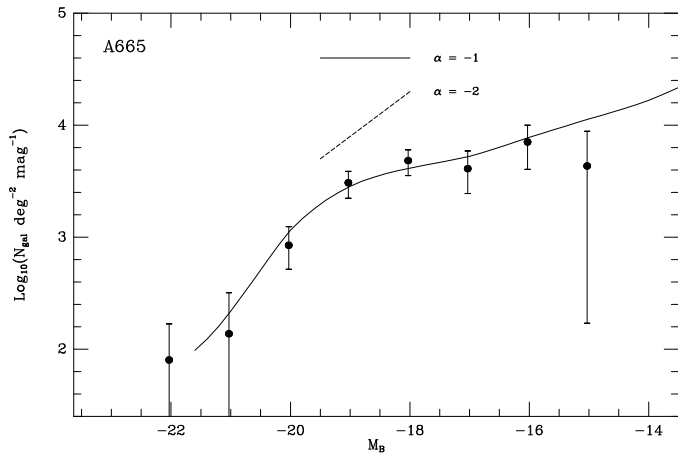


Table 1
The composite luminosity function

M_B	Environments	$\log_{10} N$ (gal deg $^{-2}$ mag $^{-1}$)	α
-22	1-15	$0.531^{+0.217}_{-0.452}$	—
-21	1-15	$1.000^{+0.134}_{-0.194}$	$-2.64^{+0.25}_{-0.36}$
-20	1-15	$1.724^{+0.062}_{-0.072}$	$-2.17^{+0.14}_{-0.16}$
-19	1-15	$2.114^{+0.038}_{-0.042}$	$-1.61^{+0.08}_{-0.09}$
-18	1-15	$2.276^{+0.033}_{-0.036}$	$-1.33^{+0.06}_{-0.07}$
-17	1-15	$2.382^{+0.033}_{-0.036}$	$-1.35^{+0.06}_{-0.05}$
-16	1,3-13,15	$2.551^{+0.029}_{-0.031}$	$-1.43^{+0.10}_{-0.09}$
-15	4-9,12,15	$2.716^{+0.081}_{-0.100}$	$-1.42^{+0.13}_{-0.11}$
-14	4-9,12,15	$2.881^{+0.090}_{-0.114}$	$-1.47^{+0.22}_{-0.20}$
-13	5-9,12	$3.124^{+0.129}_{-0.184}$	$-1.62^{+0.30}_{-0.25}$
-12	5-9,12	$3.383^{+0.170}_{-0.283}$	$-1.84^{+0.49}_{-0.36}$
-11	8,9,12	$3.859^{+0.226}_{-0.498}$	—

Environments: (1) A665; (2) A963; (3) A1146; (4) A1795; (5) Coma core ($r < 200$ kpc); (6) Coma outskirts ($r > 200$ kpc); (7) A2199; (8) A1367; (9) A262; (10) Virgo; (11) Fornax; (12) NGC 507 Group; (13) Ferguson-Sandage poor groups; (14) Tully 6 nearest groups; (15) Local Group

Environments (1) through (9) and (12) come from Trentham (1997). The data in (10) comes from Sandage et al. (1985); only data brighter than $M_B = -16$ are used in deriving the composite luminosity function, as data from Impey et al. (1988) suggest that the Sandage et al. luminosity function is incomplete fainter than this. We also exclude the photographic data of (11) and (13) fainter than $M_B = -16$ when deriving the composite luminosity function, for the same reason. The data in (11) and (13) come from Ferguson (1989) and Ferguson & Sandage (1991). The data in (14) are from Tully (1988); all data brightward of his completeness limit are included. The data in (15) are from van den Bergh (1992), converted to B magnitudes using the NED extragalactic database and estimates from the stellar population boxes of Hodge (1989). Only data brightward of the estimated completeness limit ($M_B = -13.5$, the magnitude of the recently discovered Sagittarius dwarf), are included in deriving the composite luminosity function.

Results are based on $H_0 = 75$ km s $^{-1}$ Mpc $^{-1}$ and $\Omega_0 = 1$.

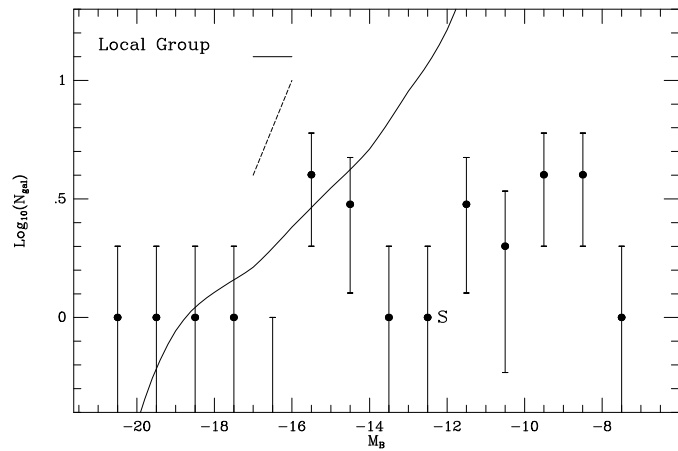
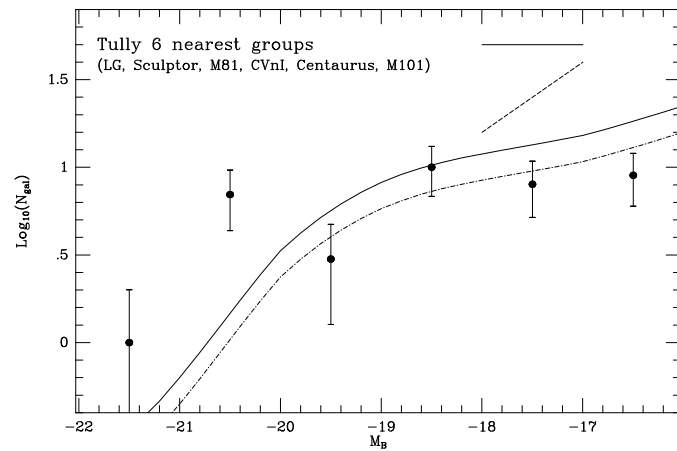
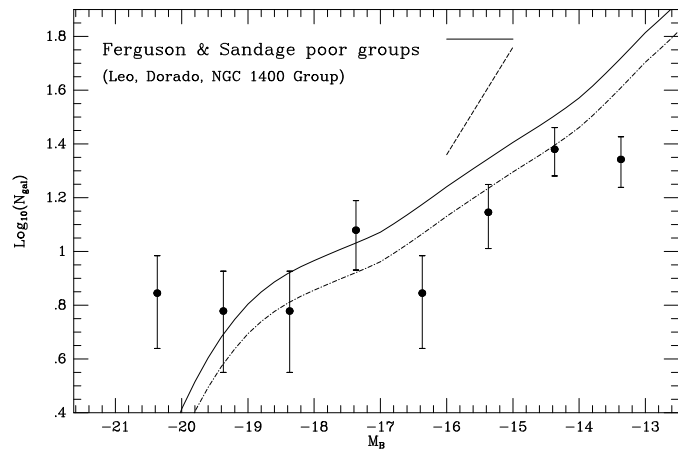
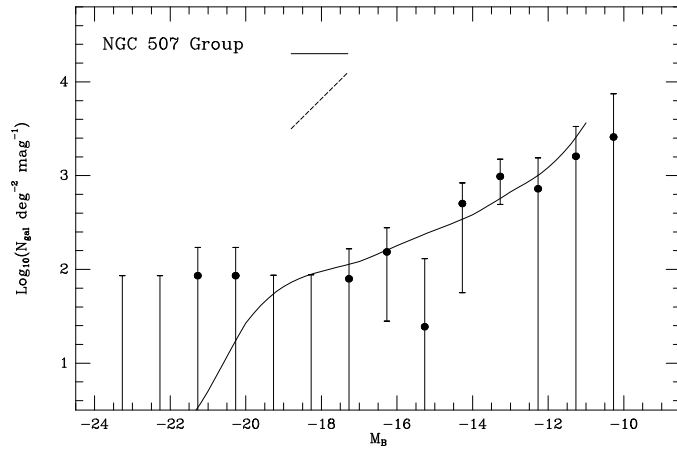
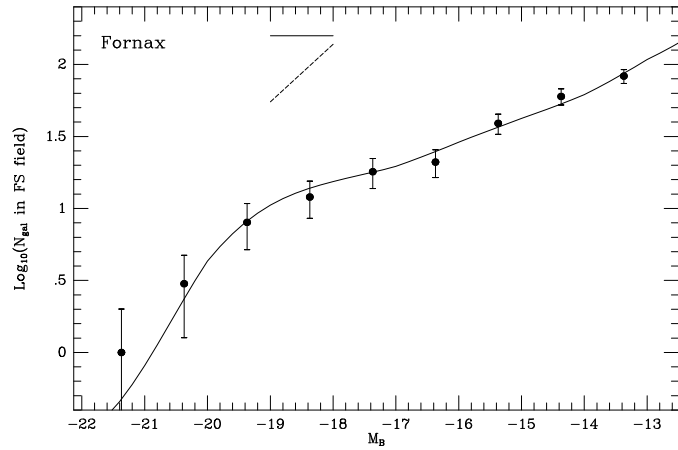
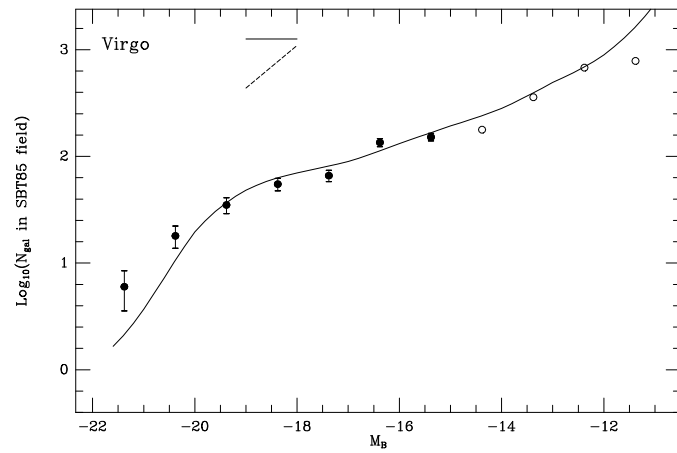
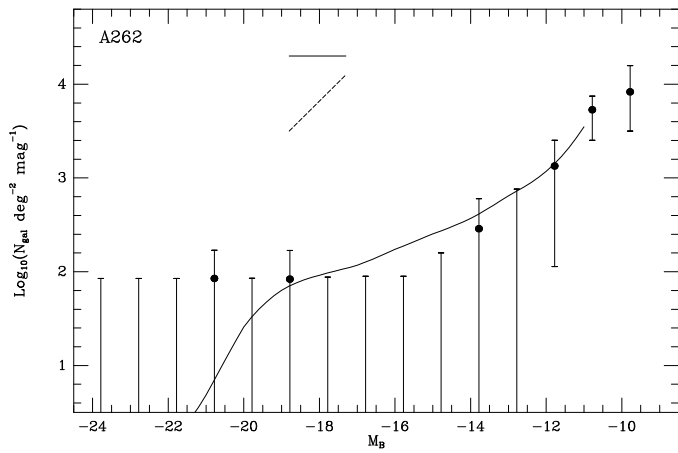


Table 2

Goodness of fit parameters for each environment
 $\phi(L)$ with $-22 < M_B < -11$

Environment	Degrees of Freedom ν	$\frac{\chi^2}{\nu}$	P
A665	6	0.17	98
A963	5	0.12	98
A1146	6	0.15	98
A1795	8	0.20	99
Coma $r < 200$ kpc	10	0.52	88
Coma $r > 200$ kpc	10	0.65	78
A2199	10	0.44	96
A1367	11	0.88	56
A262	11	0.65	79
Virgo	6	0.35	91
Fornax	6	0.46	84
NGC 507 Group	11	0.83	61
Ferguson-Sandage poor groups excluding $M_B = -20.4$ point	6 5	6.06 1.59	< 0.1 16
Tully 6 nearest groups excluding $M_B = -20.5$ point	5 4	7.51 2.10	< 0.1 8
Local Group	8	2.30	1.9

